Preliminary Chamber Measurements and a Status Report on the Development of an All-Digital Mobile Phased Array Radar

M. Yeary, R. Palmer, C. Fulton, J. Salazar-Cerreno, and H. Sigmarsson
Advanced Radar Research Center (ARRC)
University of Oklahoma, Norman, Oklahoma, USA
{yeary,fulton,rpalmer,salazar,h.sigmarsson}@ou.edu

***Abstract*— This brief manuscript provides an update on an S-band, digital-at-every-element polarimetric phased array radar designed to operate in the 2.7 – 3.1 GHz frequency band, which is being designed and built at the University of Oklahoma's Advanced Radar Research Center (ARRC). This is radar build 1 of 2 for our group in the S-band. We are currently exploring a variety of near-field panel measurements, which are presented in this paper. For instance, given that digital at every element affords vast array flexibility, new innovative concepts associated with mutual coupling calibration are being tested and verified.**

Keywords—antenna, array, digital radar, digital beamforming, phased array, polarimetric.

I. Introduction

A mobile, S-band, dual-polarized phased array system is currently under development by the ARRC [1-4], as depicted in Fig. 1. The design employs a tileable architecture, whereby each tile is comprised of a standalone 8 element x 8 element panel. Each element is dual polarized, with an independent digital waveform generator and independent digital receiver on each of the element's horizontal (H) and verticle (V) channels. Element-level digital beamforming is a goal that has been sought after for many years by a variety of research groups. Actual deployments are limited, but include: Australia's CEAFAR naval radar [5], the US Navy's FlexDAR radar, Space Fence [6], the UK's SAMPSON, Elta's MF-STAR [7] and others. Recently, other researchers are making contributions at the device level or low-channel count prototype level to achieve this, which include [8-10]. Recently, the goal of the former DARPA Arrays at Commercial Timescales (ACT) program was to develop a common technology base for electronically scanned array (ESA) systems. Under this program and partnered with Rockwell-Collins, the OU team and Rockwell-Collins were successful at developing a prototype IMPACT (Integrated Multi-use Phased Array Common Tile) to migrate towards a fundamentally digital architecture [11,12,13]. As a result, RF beamformers, down-converters, digitizers, equalizers, and some of the T/R module functionality were located within the IMPACT module to enable a more flexible FPGA-based digital backbone for the array.

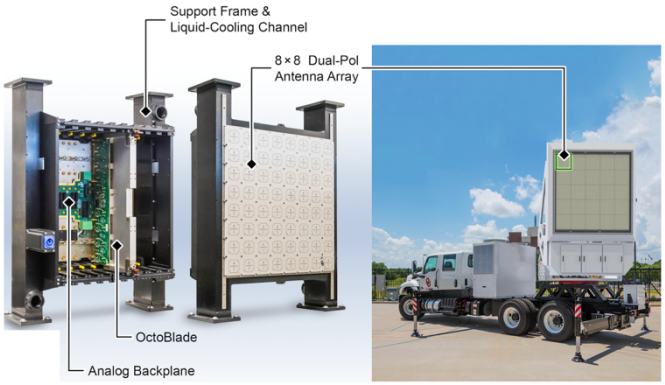

Fig. 1: On the left an 8 x 8 element array panel, on the right the full array of 32x32 elements on an S-Band Mobile Radar.

To provide some background: over the last 15 years, the ARRC has been engaged in the national Multifunction Phased Array Radar (MPAR) initiative, and subsequently the Spectrum Efficient National Surveillance Radar (SENSR) Program, as initially coordinated by the Federal Aviation Administration (FAA), the Department of Defense (DoD), the Department of Homeland Security (DHS) and the National Oceanic and Atmospheric Administration (NOAA). Consequently, the ARRC is developing two scalable all-digital polarimetric S-band phased array radars for mobile applications. The arrays support a variety of operational radar modes, including Multiple-Input and Multiple-Output (MIMO) modes, mutual coupling calibration, etc. The next section discusses our current work for the 2.7 – 3.1 GHz system, which leverages the team's experience, e.g. [14]-[23].

II. Architecture

The mobile radar depicted in Fig. 1 has a fully digital architecture, and this system will consist of 1024 elements divided into 16 panels. Each panel each houses eight "OctoBlades," and each OctoBlade supports eight dual-pol antenna elements. In brief, each OctoBlade is a line replaceable unit, and the left portion of Fig. 1 depicts the placement of one OctoBlade within a panel. Fig. 2 depicts an Octoblade, and each OctoBlade drives an eight-element column of the panel's high-performance antenna array with nearly ideal polarization

2022 IEEE Radar Conference (RadarConf22) | 978-1-7281-5368-1/22/$31.00 ©2022 IEEE | DOI: 10.1109/RADARCONF2248738.2022.9764351

along the principal planes, consisting of a metal cooling plate with PCBs on each side to house a total of 16 GaN-based frontends (> 10W per element, per polarization), eight dual-channel digital transceivers from Analog Devices, four front-end FPGAs for processing, and two FPGAs for control. In summary, with each panel having 64 elements (8x8), thus 16 panels results in 1024 total radiating/receiving elements.

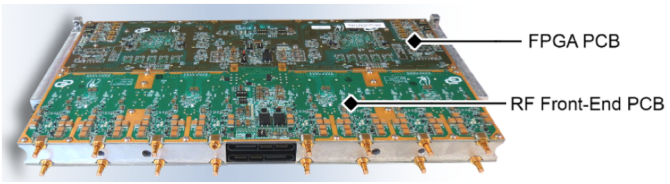

Fig. 2: Sideview of an OctoBlade. Blind-mate connectors that interface with the antenna are depicted in the foreground.

As depicted in Fig. 2, half of each OctoBlade principally contains the RF electronics, while the other half contains the FPGAs. These two halves are separated by multi-pin connectors so that independent upgrades can be conveniently supported as needed. The FPGA board is the data processing backbone of the Horus system. It integrates the functionality of several COTS FPGA boards and custom adapters into the compact OctoBlade form factor. The board has local DC power conversion, monitoring, and sequencing (single DC rail operation). Its design incorporates two powerful Arria 10 FPGAs (model 10AX 057N2 F40E2SG). Each are clocked at the component's desired maximum frequency of 275MHz. Given the targeted systems' waveform diversity requirements, algorithms will ideally be applied online, in real time and with minimal buffering and latency. Meeting these requirements ensures that the system maintains a large degree of flexibility (e.g., supporting pulse-to-pulse waveform changes) while avoiding impacts to the system's maximum pulse-repetition frequency (PRF) or other time-sensitive system-level constraints [14]. To meet these requirements, a custom solution was developed using IntelFPGA's high-level synthesis (HLS) tool to directly compute the model's output, ultimately achieving optimal throughput with relatively low resource utilization and a high F_{Max} [14].

As depicted in the foreground portions of Fig. 2, the RF Front-End PCB (with the SMA connectors) houses the GaN front-end modules (FEM), which are based on commercial, off-the-shelf (COTS) components with the exception of a moderate power GaN amplifier capable of putting out at least 10W from 2.7-3.1 GHz. Each FEM is packaged using traditional surface-mount-technology (SMT) processing, with a few bond wires and a metal top. The FEM, digital transceiver, and FPGA sections are all thermally connected through numerous thermal vias to a single, contiguous aluminum baseplate; this baseplate, in each OctoBlade, is in turn cooled by a liquid cooling path that is supported by a fractal-inspired distribution network.

At the same time, the OctoBlades are modular in the dimension normal to the array face, allowing for future exploration of different technologies at each layer; this is in contrast to a planar approach, where all of these electronics are integrated onto a single plane. This cost vs. flexibility tradeoff has been carefully considered for this particular demonstrator, and the reduced overall risk associated with a "slotted card" architecture far outweighed the benefits of a panelized approach. The direct-conversion transceivers feature on-chip FIR equalization, built-in I/Q balancing, up to 100 MHz of bandwidth, and 16-bit resolution delivering 86 dB of dynamic range – far beyond what is needed for an element-level digital radar application of this sort. The left portion of Fig. 1 depicts the relationship between an OctoBlade an a single panel.

For normal radar operation, typical digital beamforming will be accomplished over a RapidIO network feeding the back of the panels, enabling beam-bandwidth products that far exceed what would be needed for a notional multifunction system (e.g., 200-MHz beams at suitable dynamic range). To elaborate, RadioIO is a commercial open standard interface that supports high-bandwidth, low-latency, packet-switched interconnect between multiple DSP processing elements, and between DSP processing elements and bulk memory. For the Horus team, RapidIO is used to distribute the reference clock, trigger, and control to two Octoblades, and RadioIO helps to form the distributed backend of the radar.

The Horus radiating elements are designed based on the aperture-coupled stacked microstrip patch antenna with an independent polarization feed network. This radiating element enables excellent scanning performance over the frequency band (2.7 GHz to 3.1 GHz) and large e-scanning range (from -45 deg. to 45 deg). To achieve high port isolation (greater than 50 dB), and cross-polarization isolation (greater than 37 dB), the antenna was designed for perfect symmetry. In the design, the signals from the feed network are transferred using a cross-slot on a ground plane. This ground plane separates both vertical and horizontal polarization. Each feeding network is coupled to the aperture, while the aperture then couples the energy to the driven patch. More details of the antenna design and scanning performance are presented in [23].

III. Panel Measurements

The team has established a small, dedicated near-field scanner for the panels (as given by Fig. 3), while a large near-field scanner for the truck's multi-panel aperture is currently under construction. The calibration prior to the measurements is described as follows. The team performed nearfield alignment 30 consecutive times with 24 channels, performed mutual coupling alignment 30 consecutive times with 24 channels, and computed error statistics on all measured errors together to establish baseline nearfield alignment performance. Pulse parameters: 1 μs pulse, 1 pulse per CPI, 12.3 MHz offset, and

Fig. 3: Near-field panel measurement set-up. Eight OctoBlades are installed in one panel. Here, the orifice of the probe is facing the panel's aperture.

-20 dBFS transmit amplitude. Receive (RX) collections included: both polarizations, co/cross, +/- 45 deg. Cross-pol looks very nice when steered at boresight, as well as azimuth steering. Cross-pol degrades with elevation steering beyond about +/- 30 deg, and we are working on chamber improvements to rectifiy anomolies. Figs. 4(a) to 4(d) show measusrements of RX H elevation, RX V elevation, RX H azimuth, and RX V azimuth, respectively.

In addition to the traditional nearfield alignment calibration mentioned in the previous paragraph, the team has been recently working on mutual coupling calibration methods for all-digital arrays [24-28]. Consequently, Fig. 5 depicts recent Ludwig 3 AZ/EL near-field scans in receive mode (see [29] for coordinate definitions). These are among its first beamformed results, with many more expected as the system scales to its full size as OctoBlades are populated, tested, and integrated.

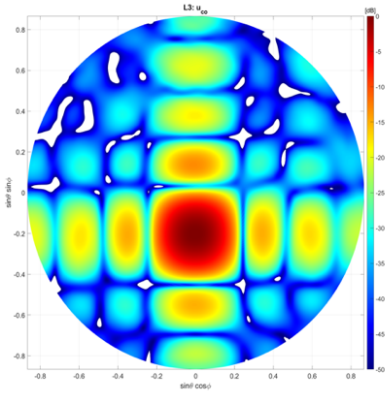

Fig. 5: Recent near-field chamber results for an 8x8 panel as depicted in Fig. 3, showing well-behaved digital beamforming after calibration.

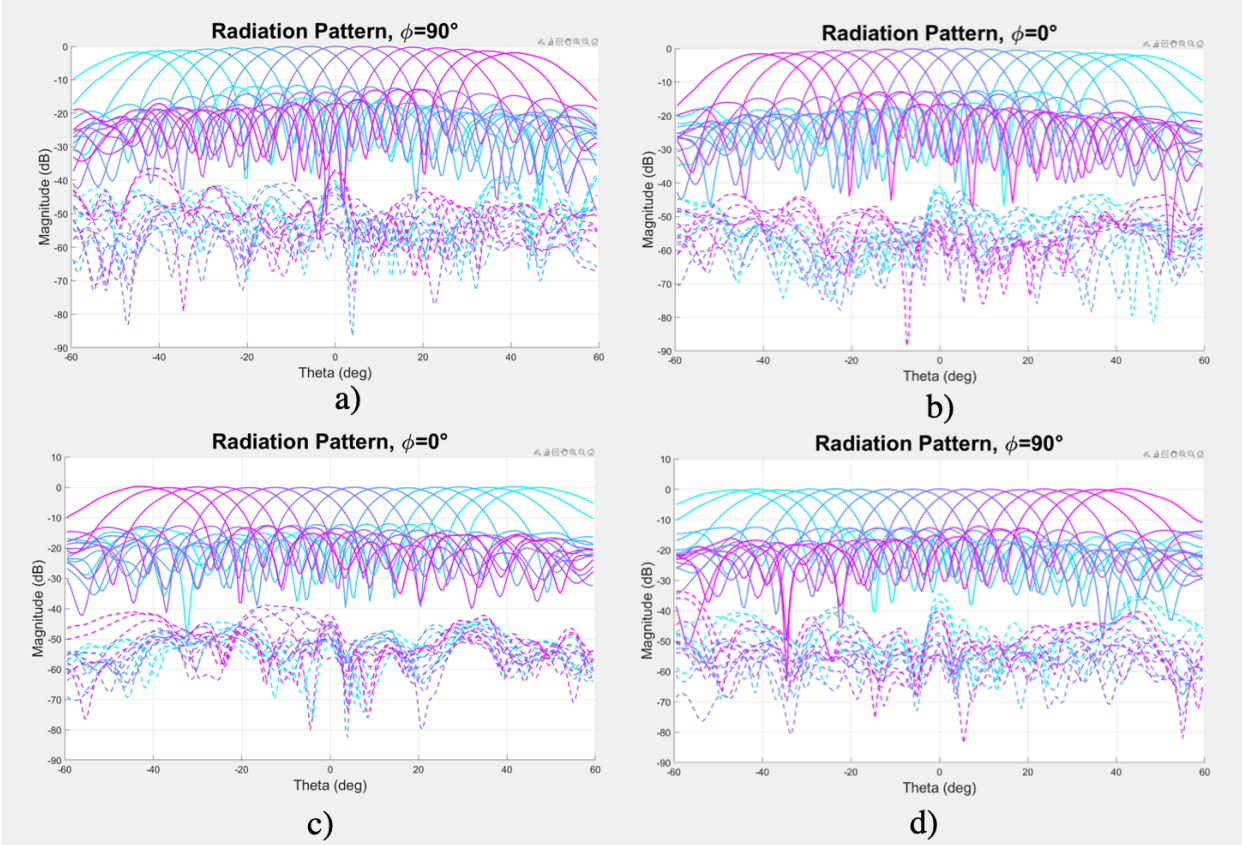

Fig. 4: a) Measured radiation patterns in reception mode for H-polarization in the elevation cut. b) Measured radiation patterns in reception mode for V-polarization in the azimuth cut. c) Measured radiation patterns in reception mode for H-polarization in the azimuth cut. d) Measured radiation patterns in reception mode for V-polarization in the azimuth cut.

Testing was also performed to assess the impact of the presence of the nearfield probe on mutual coupling calibration, mainly to determine if it had any impact. The errors appear to be reasonably small, but enough to warrant avoidance if possible (examples shown in Figs. 6 and 7).

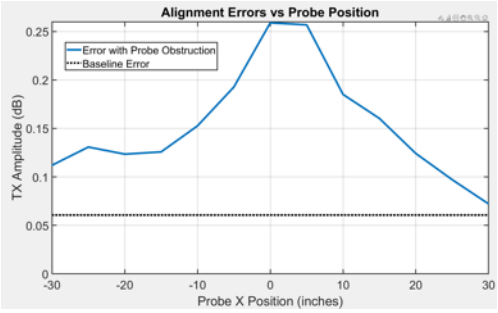

Fig. 6: TX mode – impact of the presence of the nearfield probe on mutual coupling calibration.

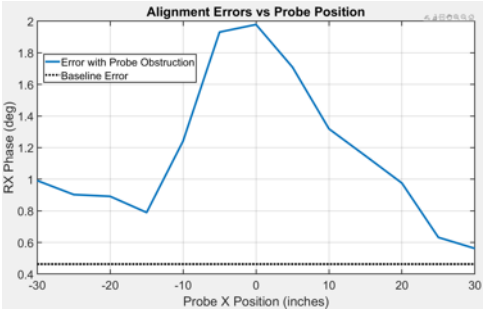

Fig. 7: RX mode – impact of the presence of the nearfield probe on mutual coupling calibration.

For mutual coupling calibration, it was found that higher transmit powers lead to calibration errors that are as much as doubled, and this is being investigated further. Saturated receivers are suspected. An approach akin to a phase-noise metric has been used to filter out saturated receivers from the overall coupling matrix, leading to better results in initial testing. It has been proven that alignment can be restored using our mutual coupling approach after power cycling the entire system following several iterations to resolve phase ambiguities. This is still under development.

III. Summary

This short conference paper provides an update on a mobile radar that is under construction at the University of Oklahoma. It is unique since it allows fully-polarimetric TX and RX at every channel to support these primary functions: radar, communications, real-time calibration, etc. Based on the fact that COTS components are highly utilized principally by the communications industry, it is the world's first large scale (>1000 elements) polarimetric, fully-digitized phased array radar system using mass market components. A brief summary of possibilities for demonstrations with the Horus system: advanced aperture and waveform agility, performing many different tasks/objectives simultaneously; multiple input multiple output (MIMO) radar, given multiple transmit and receive antennas; and exquisite control of polarimetry, such as single H, single V, simultaneous H&V for slant 45, LHC, RHC, or arbitrary polarization states. While currently the system is under development as a prototype, it is expected that this all-digital system will provide a demonstration platform for studies in (1) polarimetric phased array measurements, (2) advanced waveforms and beamforming, (3) polarimetric calibration techniques, and (4) level of digitalization, etc. It is expected that this research system can be used as a baseline for investigations of manufacturability, production costs, power consumption, and other issues.

Acknowledgement

This material is based upon research supported by, or in part by, the U. S. Office of Naval Research under award number N00014-18-1-2896 and N00014-19-1-2326. We also appreciate the initial partial funding provided by NOAA/Office of Oceanic and Atmospheric Research under NOAA-University of Oklahoma Cooperative Agreement #NA11OAR4320072, U.S. Department of Commerce. This paper is also based upon research supported by, or in part by the University of Oklahoma and the Army Research Laboratory under Agreement #W911NF-19-2-0048. The views, opinions expressed, and/or findings contained in this report are those of the authors(s), do not necessarily represent the opinions of the U.S. Government and should not be construed as an official US Government position, policy, or decision, unless so designated by other documentation. Special thanks to the ARRC's engineering staff for their dedication to the project.

References

[1] M. Yeary, R. Palmer, C. Fulton, J. Salazar, and H. Sigmarsson, "Recent Advances on an S-band All-Digital Mobile Phased Array Radar," *IEEE International Symposium on Phased Array Systems & Technology*, 2019.

[2] R. Palmer, C. Fulton, J. Salazar, H. Sigmarsson, and M. Yeary, "The "Horus" Radar An All-Digital Polarimetric Phased Array Radar for Multi-Mission Surveillance," *American Meteorological Society Annual Meeting*, session 8A.6, Phoenix, AZ, 2019.

[3] M. Yeary, R. Palmer, C. Fulton, J. Salazar, and H. Sigmarsson, "Update on an S-band All-Digital Mobile Phased Array Radar," *IEEE Radar Conference*, 2021.

[4] C. Fulton, R. Palmer, M. Yeary, J. Salazar, H. Sigmarsson, M. Weber, A. Hedden, "Horus: A testbed for fully digital phased array radars", *Microwave Journal*, invited paper, vol. 63, no. 1, pp. 20-36, January 2020.

[5] I. Croser, "Phased array technology in Australia," *IEEE A&E Systems Magazine*, pp. 24–28, 2009.

[6] J. Haimerl and G. Fonder, "Space fence system overview," *IEEE Phased Array Systems &Technology (PAST) Symposium*, pp. 1–11, 2016.

[7] I. Lupa, "History and progress of phased array developments at ELTA-IAI," *IEEE Phased Array Systems & Technology (PAST) Symp.*, 2016, plenary speaker, see document #148 on conf CD.

[8] M. Morton, Y. Chen, A. Molnar, E. Szoka, and R. Ying, "The RF Sampler: Chip-scale frequency conversion and filtering enabling affordable element-level digital beamforming," *IEEE BiCMOS and Compound Semiconductor Integrated Circuits and Technology Symposium* (BCICTS), pp. 1-5, 2018.

[9] W. Weedon, and R. Nunes, "Low-cost wideband digital receiver/exciter (DREX) technology enabling next-generation all-digital phased arrays," *IEEE International Symposium on Phased Array Systems and Technology (PAST)*, pp. 1-5. IEEE, 2016.

[10] D. Rabideau, R. Galejs, F. Willwerth, and D. McQueen, "An S-band digital array radar testbed," *IEEE International Symposium on Phased Array Systems and Technology, 2003.*, pp. 113-118, 2003.

[11] T. Hoffmann, C. Fulton, M. Yeary, A. Saunders, D. Thompson, B. Murmann, B. Chen, and A. Guo, "IMPACT – A common building block to enable next generation radar arrays," *IEEE Radar Conference*, pp. 1-4. 2016.

[12] T. Hoffmann, C. Fulton, M. Yeary, A. Saunders, D. Thompson, B. Murmann, B. Chen, and A. Guo, "Measured performance of the IMPACT common module – a building block for next generation phase arrays," *IEEE International Symposium on Phased Array Systems and Technology* (PAST), pp. 1-7, 2016.

[13] L. Paulsen, T. Hoffmann, C. Fulton, M. Yeary, A. Saunders, D. Thompson, B. Chen, A. Guo, and B. Murmann, "Impact: a low cost, reconfigurable, digital beamforming common module building block for next generation phased arrays," vol. 9479, pp. 1-15, *Proc. of SPIE*, 2015.

[14] M. Herndon and M. Yeary, "Real-Time FPGA-based Digital Predistortion for Improved Amplifier Performance in Next Generation Phased Arrays," *IEEE Radar Conference*. NYC, March 21-25, 2022.

[15] J. Salazar, D. Schvartzman, D. Bodine, R. Palmer, J. McDaniel, M. Yeary, N. Aboserwal, B. Cheong, and T.-Y. Yu, "A design approach for a dual-Doppler Ka-band mobile radar architecture with rapid-scanning volumetric imaging for Earth systems science," *IEEE Radar Conference*. NYC, March 21-25, 2022.

[16] C. Fulton, M. Yeary, D. Thompson, J. Lake, and A. Mitchell, "Digital phased arrays: Challenges and opportunities," *Proceedings of the IEEE*, invited paper, vol. 104, no. 3, pp. 487-503, 2016.

[17] B. Isom, R. Palmer, R. Kelley, J. Meier, D. Bodine, M. Yeary, B. Cheong, Y. Zhang, T.-Y. Yu, M. Biggerstaff, "The atmospheric imaging radar: simultaneous volumetric observations using a phased array weather radar," *Journal of Atmospheric and Oceanic Technology*, vol. 30, no. 4, pp. 655-675, April 2013.

[18] C. Fulton, J. Salazar, D. Zrnic, D. Mirkovic, I. Ivic, and R. Doviak, "Polarimetrie phased array calibration for large-scale multi-mission radar applications," *IEEE Radar Conference* (RadarConf18), pp. 1272-1277, April 2018.

[19] N. Peccarelli, B. James, R. Irazoqui, J. Metcalf, C. Fulton, and M. Yeary, ``Survey: characterization and mitigation of spatial/spectral interferers and transceiver nonlinearities for 5G MIMO systems," *Transactions on Microwave Theory and Techniques – Special Issue on 5G*, vol. 67, no. 7, pp. 2829-2846, July 2019. DOI: 10.1109/TMTT.2019.2914382

[20] M. Yeary, J. Crain, A. Zahrai, C. Curtis, J. Meier, R. Kelley, I. Ivic, R. Palmer, D. Doviak, G. Zhang, and T.-Y. Yu, "Multi-Channel Receiver Design, Instrumentation, and First Results at the National Weather Radar Testbed," *IEEE Transactions on Instrumentation and Measurement*, vol. 61, no. 7, pp. 2022-2033, July 2012.

[21] B. Isom, R. Palmer, R. Kelley, J. Meier, D. Bodine, M. Yeary, B. Cheong, Y. Zhang, T.-Y. Yu, M. Biggerstaff, "The atmospheric imaging radar: simultaneous volumetric observations using a phased array weather radar," *Journal of Atmospheric and Oceanic Technology*, vol. 30, no. 4, pp. 655-675, April 2013.

[22] R. Palmer, et al., "Transportable phased array radar: Meeting weather community needs, *AMS Annual Meeting*, Houston, TX, 2022.

[23] J. D. Díaz et al., "A Cross-Stacked Radiating Antenna With Enhanced Scanning Performance for Digital Beamforming Multifunction Phased-Array Radars," in IEEE Transactions on Antennas and Propagation, vol. 66, no. 10, pp. 5258-5267, Oct. 2018, doi: 10.1109/TAP.2018.2862252.

[24] J. Lujan, C. Fulton, M. Yeary, E. Langley, S. McCormick, and A. Hedden, "Phased array radar initial alignment algorithm using mutual coupling: an iterative approach," *Radar Sensor Technology XXIV*, vol. 11408, p. 1140811, *International Society for Optics and Photonics*, 2020.

[25] N. Peccarelli, and C. Fulton. "A mutual coupling approach to digital pre-distortion and nonlinear equalization calibration for digital arrays," *IEEE International Symposium on Phased Array System & Technology* (PAST), pp. 1-8, 2019.

[26] R. Lebrón, P.-S. Tsai, J. Emmett, C. Fulton, and J. Salazar-Cerreno, "Validation and testing of initial and in-situ mutual coupling-based calibration of a dual-polarized active phased array antenna," *IEEE Access* 8 (2020): 78315-78329.

[27] M. Herndon, M. Yeary, and R. Palmer, "Studies of front-end distortion characterization via mutual coupling measurements in phased array systems," *IEEE International Radar Conference,* pp. 798-803, April, 2020.

[28] C. Fulton, J. Salazar, Y. Zhang, G. Zhang, R. Kelly, J. Meier, M. McCord, D. Schmidt, A. Byrd, L. M. Bhowmik, S. Karimkashi, D. Zrnic, R. Doviak, A. Zahrai, M. Yeary, and R. Palmer "Cylindrical polarimetric phased array radar: Beamforming and calibration for weather applications," *IEEE Transactions on Geoscience and Remote Sensing,* vol. 55, no. 5, pp. 2827-2841, May 2017.

[29] G. F. Masters and S. F. Gregson, "Coordinate system plotting for antenna measurements," *AMTA Annual Meeting & Symposium*, vol. 32, 2007.